Accelerated insulin aggregation under alternating current electric fields: Relevance to amyloid kinetics

Zhongli Zheng,[1] Benxin Jing,[1] Mirco Sorci,[2] Georges Belfort,[2] and Yingxi Zhu[1,a)]
[1]*Department of Chemical and Biomolecular Engineering, University of Notre Dame, Notre Dame, Indiana 46556, USA*
[2]*Howard P. Isermann Department of Chemical and Biological Engineering and The Center for Biotechnology and Interdisciplinary Studies, Rensselaer Polytechnic Institute, Troy, New York 12180, USA*

(Received 7 July 2015; accepted 7 August 2015; published online 25 August 2015)

The time-dependent nucleation phase is critical to amyloid fibrillation and related to many pathologies, in which the conversion from natively folded amyloidogenic proteins to oligomers via nucleation is often hypothesized as a possible underlying mechanism. In this work, non-uniform AC-electric fields across two asymmetric electrodes were explored to control and examine the aggregation of insulin, a model amyloid protein, in aqueous buffer solution at constant temperature (20 °C) by fluorescence correlation spectroscopy and fluorescence microscopy. Insulin was rapidly concentrated in a strong AC-field by imposed AC-electroosmosis flow over an optimal frequency range of 0.5–2 kHz. In the presence of an AC-field, direct fibrillation from insulin monomers without the formation of oligomer precursors was observed. Once the insulin concentration had nearly doubled its initial concentration, insulin aggregates were observed in solution. The measured lag time for the onset of insulin aggregation, determined from the abrupt reduction in insulin concentration in solution, was significantly shortened from months or years in the absence of AC-fields to 1 min–3 h under AC-fields. The ability of external fields to alter amyloid nucleation kinetics provides insights into the onset of amyloid fibrillation. [http://dx.doi.org/10.1063/1.4928767]

INTRODUCTION

Amyloid fibrillation has been extensively studied both *in vivo* and *in vitro*[1–3] due to its association with more than twenty-five neurogenerative diseases including Huntington's disease, Parkinson's disease, bovine spongiform encephalopathy, and Alzheimer's disease.[4–12] However, the molecular origin underlying these diseases remains debated without conclusive agreement. One school has proposed two routes to nucleation—one primary or inherent and the other secondary from fibril breakage.[13] As a result, Ferrone[14] posits that monomers conformationally fold into the nucleus. Others have focused on assembly dynamics of amyloid fibrils involving a conformational transition from soluble native folded forms to long β-sheet rich fibrils in a sigmoidal time-dependent process that includes a rate limited nucleation phase and a subsequent fibril growth phase.[15–20] Conversely, different oligomer forms of secondary nucleation, rather than a primary one from a single independent nucleus, have been recently reported.[21–23] Additionally, it has been found that many amyloid fibrils exist in nature, termed "functional amyloid," exhibiting a function seemingly unrelated to diseases but rather to normal biological activity.[6,24–26] Thus, understanding an *in vitro* control of amyloid fibrillation has great implications for biomaterial syntheses and biomedical aspects.

a)Author to whom correspondence should be addressed. Electronic mail: yzhu3@nd.edu.

To elucidate the underlying mechanism of amyloid fibrillation, it is important to be capable of controlling or altering the lag phase involving time-dependent amyloid protein nucleation. The aggregation of soluble native protein into amyloid fibrils can be accelerated *in vitro* by changing solution temperature[1] or pH[27] or can be delayed by the addition of inert solutes.[28] One approach to vary the nucleation reaction rate is to employ external electric field. The focus of this study is to explore non-uniform AC–electric fields to control the lag phase in protein aggregation, which could shed light to currently debated mechanisms of amyloid fibrillation. As it remains unclear whether conformational conversion is accompanied by protein aggregation in these *in vitro* studies[1,25,28] and different oligomers could be formed, experimental characterization also demands spatial and temporal resolution.

In this work, we investigated the aggregation process of insulin, a model amyloid protein, under an imposed non-uniform AC-electric field of varied field frequency and voltage by ultrafast fluorescence correlation spectroscopy (FCS) at a single molecule level and fluorescence microscopy. Using an AC-electric field is a simple and versatile approach to effectively and reversibly manipulate the conformational structure of polyelectrolytes.[29] This avoids undesired electrode redox effects due to a DC-electric field. It was theoretically predicted that the energy landscape between distinct macromolecular structures can be modulated by applied AC-fields, thereby leading to the effective control of supramolecular aggregation.[29,30] Recently, ac-electric fields have been successfully employed to produce single protein crystals in an aqueous solution.[30] Here, we focus on the effects of an AC-electric field on the nucleation rate of insulin protein in aqueous solution at room temperature. Insulin is a small, well-folded protein[31,32] and can form long amyloid-like fibrils under denaturing conditions such as low pH, high temperature, and high ionic strength.[33–35] For instance, insulin fibril formation can take place after a lag time of 2–3 h,[33,34] in a buffer solution of pH = 2 at T = 65 °C in contrast to a lag time of months or even years at human body temperature (T ≈ 37 °C). Additionally, instead of using ensemble-averaged characterization methods, such as UV-spectroscopy and circular dichroism to determine the aggregation kinetics or atomic force microscopy (AFM) and TEM to characterize equilibrium structures, without sufficient temporal resolution,[33,34] we use FCS to examine the aggregation process of insulin proteins *in-situ* with applied AC-fields of varied frequency and voltage at a single-molecule level. FCS allows accurate measurement of insulin structural change at a single protein level or at a probe protein concentration of 10^{-9} M, which is three orders of magnitude lower than that required for many ensemble-averaged methods such as turbidity and circular dichroism measurements. Additionally, the temporal resolution of our FCS is on the order of sub-micrometer second,[36] comparable to the applied AC-frequency range of 0.5 kHz–100 kHz in this work, thereby allowing *in-situ* characterization of AC-field induced insulin structural dynamics.

EXPERIMENTAL

Materials and sample preparation

Human recombinant insulin of molecular weight 5808 Da with 51 amino acids in two linked amino acid chains by disulphide bonds is obtained from Novo Nordisk A/S, Denmark. Fluorescence probe, 5-carboxyrhodamine 6G succinimidyl ester (5-CR6G), is purchased from Invitrogen and used as directed. Sodium chloride, sodium acetate, and acetate acid in analytical purity are all purchased from Sigma-Aldrich. Deionized water used in this work is purified by a Barnstead Nanopure II system.

2.0 mg/ml plain insulin solution is prepared in aqueous buffer solution containing 0.1 mol/l (M) sodium acetate and 20% acetate acid in deionized water to pH = 2.74, similar with the experimental condition reported in the literature,[37] yielding the medium conductivity of 5.7 S/m. To ensure that insulin is in the same structure without aggregation, pH cycling is conducted with the stock insulin solution before each experiment.[37] 5-CR6G probe is attached to the C (or N) terminal end of insulin by following the typical protein labeling protocol.[38] For FCS experiments, 5-CR6G labeled insulin at an extremely low concentration of 3.5×10^{-9} M is added to plain insulin aqueous solution. For fluorescence microscopic experiments, 1.0 mol.

% 5-CR6G labeled insulin mixed with plain insulin is added to the buffer solution of total 2.0 mg/ml insulin. All the solutions are filtered through a filter of diameter 0.22 μm (Fisher Scientific) before experiments.

All the glass coverslips (Fisher Scientific) and quartz coverslips (ESCO Products) used in our experiments are first cleaned in a heated piranha solution (30 vol. % H_2O_2 and 70 vol. % H_2SO_4) at T = 120 °C for 1 h. For electrode fabrication, clean glass coverslips are first deposited with a 30 nm thick titanium layer to enhance the gold bonding with the substrate and followed by a gold layer of 1 μm thick by E-beam evaporation (FC1800), both at a deposition speed of 0.2 nm/s to ensure the smoothness and homogeneity of deposited metal films.

Experimental setup

All the experiments are conducted using a microchannel embedded with two parallel gold-coated glass coverslips as illustrated in Figure 1(a). The top electrode surface is fully covered with gold. The bottom electrode surface is only half coated with gold of the same thickness as the top one, while the other half surface is bare glass. The two parallel electrode surfaces are separated by a gap spacing of $L = 0.5$ mm using insulating rubber spacers and assembled into a microfluidic channel. Two electrode surfaces are connected via copper tapes and wires with alligator clips to a function generator (Stanford Research System). Square waveform electric potential of varied peak-to-peak voltage, $V_{pp} = 5$–80 V, and frequency, $\omega = 0.5$–100 kHz, was applied across two electrodes. The electric circuit connection and output waveform across two electrodes are verified by a digital multi-meter (Protek 506) and an oscilloscope (Tektronix TSD1001B).

We have calculated the distribution of electric field intensity between two electrodes by COMSOL Multiphysics. As shown in Figure 1(b), the applied AC-electric potential in a square waveform across two asymmetric electrodes produces a non-uniform AC-electric field, in which a strong field region is located near the edge of bottom electrode interfaces, while a weak field

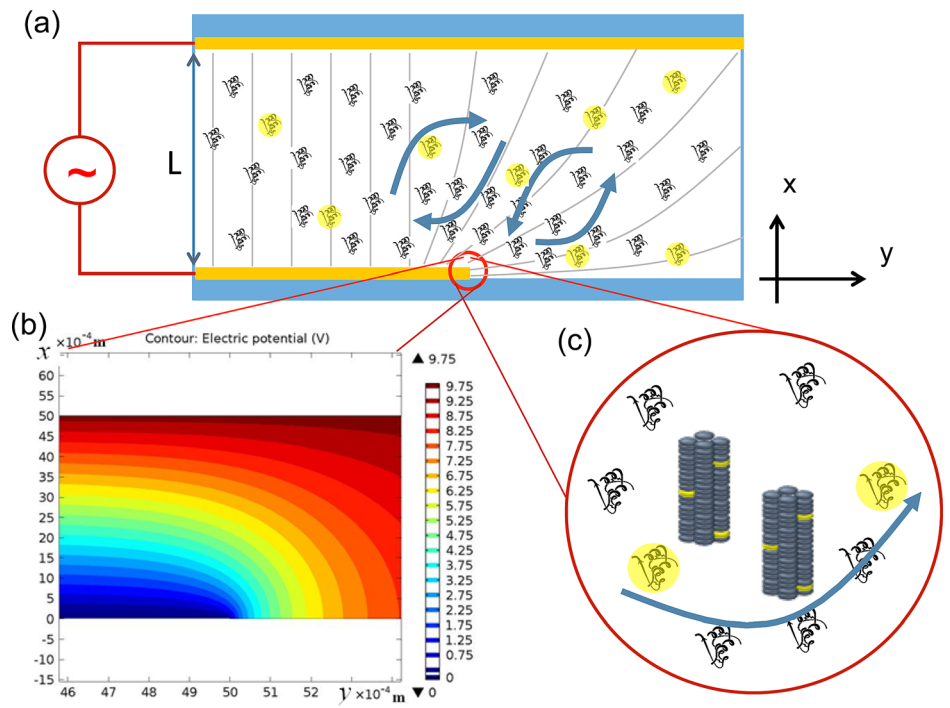

FIG. 1. (a) Schematic illustration of experimental setup and applied AC-field lines. The circle in (a) indicates the location of the laser focus spots in the FCS and CLSM experiments, (b) simulated profile of AC-electric field potential in the circled area versus distance from the bottom electrode surface by COMSOL Multiphysics, and (c) schematic illustration of applied non-uniform AC-fields induced concentration and fibrillation of insulin monomers.

region is located in the bulk solution far from the electrode interface. To avoid electrode polarization, we have limited the lowest AC-frequency to 0.5 kHz, below which undesired severe adsorption of insulin at the electrode surface is observed.

Characterization

Real-time structural dynamics of insulin in aqueous solutions in response to applied AC-electric fields is examined by one-photon FCS at a single-molecule level. FCS is set up on an inverted microscope (Zeiss, Observer Z1) equipped with an oil immersion 100× objective lens (NA = 1.4). The time evolution of AC-field induced insulin aggregations in aqueous solutions is also monitored by confocal laser scanning microscopy (CLSM) (Zeiss, Pascal 5) over an area of 90×90 μm^2 at the resolution of 512×512 pixels^2. For both FCS and CLSM experiments, the laser is focused at the edge of the bottom electrode surface corresponding to the strong electric field region, as schematically circled in Figure 1.

FCS is a sensitive and rapid method to determine molecular dynamic structures, including polymer conformations,[29] DNA hybridization,[39] and protein aggregation[40] in varied environmental conditions. Briefly, the tiny fluctuations, $I(t)$ in fluorescence intensity, due to the motion of fluorescence labeled insulin in and out of the small laser excitation volume using an Argon ion laser (Melles Griot, $\lambda_{ex} = 488$ nm), is measured by two sensitive single-photon counting modules (Hamamatsu, Model H7421-40) independently at a time interval of typically 10–100 μs in a confocal detection geometry. The auto-correlation function, $G(\tau)$ of measured $I(t)$ is thereby obtained as

$$G(\tau) = \frac{\langle \delta I(t) \delta I(t+\tau) \rangle}{\langle I(t) \rangle^2} \tag{1}$$

by cross-correlation analysis,[41–43] which removes the artifacts from detectors. The diffusion coefficient, D, and concentration, [c], of fluorescence-labeled insulin in dispersion or aggregation states are extracted by fitting $G(\tau)$ with a known transport model. Considering the flow induced by inhomogeneous AC-fields, we have fitted the normalized $G(\tau)$ by $G(\tau = 0)$ using a model[44] including both diffusion and lateral fluid net flow velocity v as

$$G(\tau) = \left([\mathrm{c}]\pi^{1.5}\varpi^2 z\right)^{-1} \left(1 + \frac{4D\tau}{\varpi^2}\right)^{-1} \left(1 + \frac{4D\tau}{z^2}\right)^{-0.5} \exp\left[\left(-\frac{\tau v}{\varpi}\right)^2 \left(1 + \frac{4D\tau}{\varpi^2}\right)^{-1}\right], \tag{2}$$

where $\varpi \approx 276$ nm and $z \approx 3$ μm are the respective lateral and vertical dimensions of our FCS excitation focal volume and calibrated by Rhodamine 6G dye of a well-known D ($= 420$ μm^2/s) in a dilute aqueous solution.[45] The experimental uncertainty on measured D and [c] with FCS is about 20%. A control experiment has confirmed that $D \approx 179$ μm^2/s for 5-CR6G labeled insulin monomer can be clearly differentiated from free 5-CR6G of measured $D \approx 420$ μm^2/s in buffer solution at pH = 2.74.

The structure of insulin aggregates formed under applied AC-electric fields is also characterized by tapping-mode AFM (Veeco multimode with a Nanoscope IV controller) using a standard Si cantilever (TESPA) in air. The insulin aggregates are collected from the solution after the application of applied AC-electric field and diluted with deionized water. Subsequently, a sample aliquot of 20 μl is placed onto a clean silicon wafer to allow the adsorption of insulin aggregates for 10 min. The surface with adsorbed insulin was rinsed with deionized water to remove excess insulin prior to AFM acquisition.

RESULTS AND DISCUSSION

First, we employed FCS to examine the insulin aggregation in aqueous buffer at varied pH values at T = 20 °C in the absence of electric fields (control). By varying the pH up and down at T = 20 °C, the measured $G(\tau)$ normalized by $G(\tau = 0)$ changes with pH. Previously, we have

shown that pH cycling is useful for preparing homogeneous insulin solutions.[37] $G(\tau)/G(0)$ is fitted well with Eq. (2), with $v = 0$ to yield D as a function of pH. From the Stokes-Einstein relationship

$$R_H = \frac{k_B T}{6\pi\eta D}, \tag{3}$$

where k_B is the Boltzmann constant, T is kept constant at 20 °C in this work, and $\eta \approx 1.0 \times 10^{-3}$ Pa s is the viscosity of aqueous buffer solution. The hydrodynamic radius, R_H (pH), which is examined for insulin aggregation, can be estimated from D(pH). Without pH cycling, insulin obtained from the vendor was mainly in the form of hexamers of $R_H = 3.0$ nm at pH = 2.0.[46,47] As shown in Figure 2, by adding NaOH to insulin aqueous solution, R_H decreases with increasing pH, indicating the dissociation of insulin hexamers to trimers of $R_H = 2.0$ nm at pH = 3.8–9 and monomers of reported $R_H = 1.2$ nm at pH = 11.83.[46,48,49] Subsequently, adding HCl to decrease the pH from 11.83 to 1.60 only leads to a slight R_H change, which should be due to the sensitivity of insulin monomer conformation to pH value. The results reported below are all obtained with insulin samples after the pH cycling to ensure consistency of the initial insulin structure prior to application of AC-fields. We also demonstrated that FCS is sufficiently sensitive to capture the variation of insulin oligomer forms in solution.

A separate control experiment with insulin solutions at T = 65 °C in the absence of AC-electric fields was also run. Aliquots (200 μl) at different incubation times were collected and characterized with FCS. We have confirmed that a lag time for insulin aggregation prior to the onset of fibril growth under these harsh conditions (sodium chloride concentration 0.1 M, pH 1.6, and T = 65 °C) was ~2.5 h.[33,34] This was based on the observation of an abrupt reduction in measured insulin fluorescence. This also agrees with the previously reported lag time of ~2.5 h determined under similar conditions using Thioflavin T and absorbance reading at 600 nm.[33,34] Hence, FCS was able to reproduce and monitor insulin aggregation. However, there was no perceptible changes in the measured D, suggesting a lack of oligomer formation upon insulin aggregation as reported previously by Pease *et al.*[46] Hereafter, we focus on the effect of AC-electric fields on the kinetics of insulin aggregation from insulin monomers (2.0 mg/ml insulin, pH = 2.74 after pH cycling, and T = 20 °C).

During the first or lag phase of insulin conversion from monomer to oligomer to fibril, a nucleation process is considered the rate-limiting step and can be accelerated to provide a

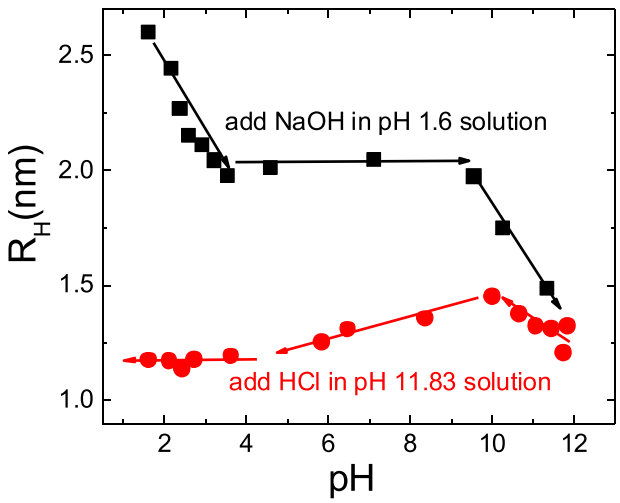

FIG. 2. The hydrodynamic radius of insulin measured in buffer solution of 2.0 mg/ml insulin. The pH was gradually increased from 1.6 to 11.83 with NaOH (black squares) and decreased with HCl (red circles). At the end of this pH cycle, the majority of the insulin molecules were monomers and used for all the subsequent experiments. The cycle also dissolves any preformed aggregates.[46] The temperature was kept constant at T = 20 °C.

shortened lag time by increasing T.[28,33,34,37] Here, we investigated the AC-electrokinetic effect on insulin aggregation in aqueous solution at constant T = 20 °C with FCS. As shown in Figure 3(a), the measured $G(\tau)$ in response to applied AC-fields in the focal area located at the edge of the bottom electrode surface exhibits little change over the range of AC-frequency, $\omega = 0.5$–10 kHz, or in the absence of AC-fields, except the value of $G(\tau)$ at short τ time scale due to the change in $G(0)$. Each $G(\tau)$ versus τ was fitted excellently with Eq. (2), yielding $D = 179 \pm 10\,\mu m^2/s$ independent of ω as shown in Figure 3(b). Accordingly, $R_H = 1.2$ nm for various ω values and suggests that no detectable oligomer was formed under applied AC-fields and that insulin remained a monomer.

As evidenced in Figure 3(a) (inset), $G(0)$ exhibits strong dependence on ω. As $G(0)$ scales inversely with $[c]\pi^{1.5}\varpi^2 z$ as shown in Eq. (2), the concentration of insulin in the focal volume, located in the strong field region near the bottom electrode, normalized by the bulk concentration of fluorescence-labeled insulin, $[c]_o = 3.5$ nM, is plotted against elapsed time in Figure 4. At various $\omega = 0.5$–2 kHz and constant $V_{pp} = 10$ V, the measured insulin concentration initially increases linearly with time, suggesting AC-field driven accumulation of insulin monomers, then exhibits an abrupt decrease down to the initial bulk concentration, $[c]_o$, and remains at a constant value over time. At $\omega \geq 5$ kHz, the effect of AC-field on accumulating insulin in the strong AC-field region seems to diminish as the concentration grows much slower over time, and no abrupt reduction in insulin concentration is observed over a 24 h time period. The critical time, upon which an abrupt reduction in insulin concentration was observed, is determined as the lag time for insulin fibrillation. Clearly, the lag time determined from the concentration profiles shows a strong dependence on ω as summarized in Table I. The lag time for insulin aggregation under applied AC-field of $\omega = 0.5$–2 kHz and $V_{pp} = 10$ V was significantly shortened to ~0.5–3 h, in comparison to a significantly longer lag time (at least >21 days in our control test) without AC-fields at T = 20 °C. Upon the abrupt decrease in insulin concentration, the precipitation of insulin aggregates from the buffer solution is observed and was collected for AFM characterization. The soluble insulin remained in the monomer form without any detectable aggregation by FCS. Hence, the results clearly indicate no conversion from insulin monomers to oligomers prior to insulin aggregation within our FCS detection limit, which agrees with the results reported by Pease *et al.*[46] The elevation of insulin concentration from the bulk by a factor of 1.5–2.5 appears to be the sole pre-requisite for insulin aggregation, which is similar to shortening the lag time by increasing initial insulin concentration.[50–52]

We attribute the accelerated lag phase of insulin aggregation to AC-electroosmosis (AC-EO) flow, which results from the action of a non-uniform AC-field on the diffusive ions in insulin solution near a polarized electrode surface.[53] The AC-EO flow imposed on an insulin

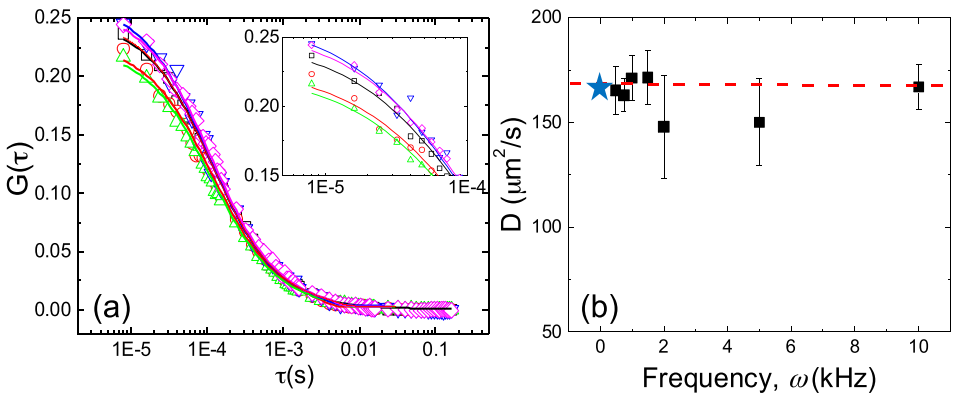

FIG. 3. (a) Auto-correlation function, $G(\tau)$, of 5-CR6G fluorescence labeled insulin in aqueous solution of pH = 2.74 in response to applied AC-field of constant $V_{pp} = 10$ V and various $\omega = 0.5$ kHz (green triangles), 1 kHz (red circles), 2 kHz (black squares), 5 kHz (blue inverted triangles), and 10 kHz (magenta diamonds). Inset: the enlargement of $G(\tau)$ at short τ. Solid lines are the fitting of $G(\tau)$ with Eq. (2). (b) Measured diffusion coefficient, D, of single insulin against ω at $V_{pp} = 10$ V by fitting $G(\tau)$ with Eq. (2), in contrast to $D = 179\,\mu m^2/s$ measured without applied AC-fields (blue star).

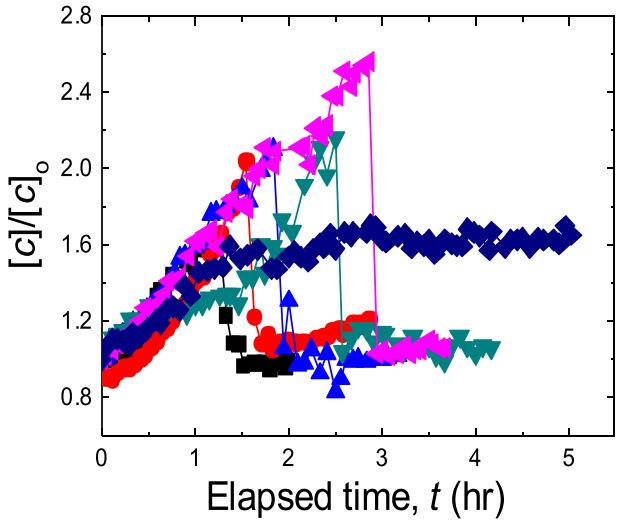

FIG. 4. Measured insulin concentration, [c], in the laser focal volume normalized by the bulk concentration, $[c]_o$, versus elapsed time under applied AC-fields of constant $V_{pp} = 10$ V and with varied $\omega = 0.5$ kHz (black squares), 0.75 kHz (red circles), 1 kHz (blue triangles), 1.5 kHz (olive inverted triangles), 2 kHz (magenta left triangles), and 10 kHz (navy diamonds). It is noted that without the AC-field, insulin concentration remains constant at $[c]_o$ as indicated by the dashed line.

solution can effectively reduce the diffusion-controlled nucleation process and enhance insulin mixing to concentrate insulin in the strong AC-field region near electrodes. AC-EO flow is predicted to peak at a characteristic frequency, $\omega_{AC\text{-}EO}$, according to the scaling theory of $\omega_{AC\text{-}EO} \sim D_{ion}/\lambda_d L$ (Eq. (3))[54,55] ~2 kHz for the insulin buffer solution, where D_{ion} is the ion diffusivity and approximately of the order of 10^{-9} m^2/s, λ_d is the Debye screening length and ~1 nm for the acetate buffer solution at pH = 2.74, and $L = 0.5$ mm is the electrode separation distance. AC-EO effect vanishes at lower and higher frequency away from $\omega_{AC\text{-}EO}$.[54,55] To quantify the AC-EO flow, we measured the time-averaged insulin velocity, v, under applied AC-fields of various ω by fitting $G(\tau)/G(0)$ with Eq. (2). As shown in Figure 5, v measured in the focal area located at the edge of the bottom electrode surface shows a strong dependence on AC-frequency and voltage. The net velocity decreases with increasing frequency range from 0.5 to 2 kHz and then flattens out at $\omega \geq 5$ kHz. Increasing applied voltage also leads to increasing net velocity linearly as shown in Figure 5 (Inset). The presence of optimal AC-field frequency in this work suggests capacitive charging induced AC-EO flow, in which AC-EO velocity scales with $V_{pp}{}^2$.[54,55] However, AC-EO flow can be also induced by Faradaic charging mechanism, in which AC-EO velocity scales with $\exp(V_{pp})$.[53] As it is difficult to exclude Faradaic charging in our electrode design, accurate scaling of AC-EO velocity with V_{pp} cannot be derived from our experimental results. Nevertheless, the lag time summarized in Table I appears to decrease with decreasing ω over the range of 0.5–2 kHz. As the decrease of lag time is accompanied by the increase of AC-EO velocity at the same AC-frequency range, an optimal AC-frequency window of 0.5–2 kHz is apparently present, which is consistent with the theoretically predicted $\omega_{AC\text{-}EO}$. Due to severe insulin adsorption and electrode oxidation at $\omega < 0.5$ Hz, the experiments at AC-frequency much lower than $\omega_{AC\text{-}EO}$ cannot be accessed. Nevertheless, approximate to the optimal AC-frequency window, insulin monomers are effectively

TABLE I. Comparison of lag time, t_{lag} measured by FCS and CLSM under applied AC-fields of constant $V_{pp} = 10$ V and varied ω.

ω, kHz	0	0.5	0.75	1	1.5	2	5
t_{lag} (FCS), h	...	1.3	1.6	2.0	2.6	3.0	>24
t_{lag}(CLSM), h	...	0.5	...	3.8	...	4.1	>24

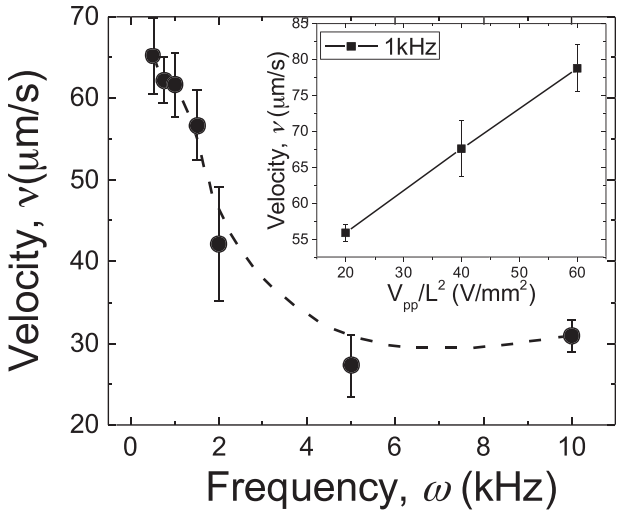

FIG. 5. Measured time-averaged velocity, v, of insulin, by fitting $G(\tau)$ with Eq. (2), against ω at constant $V_{pp} = 10$ V. Dashed line provides visual assistance. Inset: Measured time-averaged velocity, v, of insulin against V_{pp}/L^2, where L is the separation distance between two electrodes and which indicates the field gradient near the electrode surface with applied voltage.

concentrated to aggregate at much shorter lag time by AC-EO flow than the one in the absence of AC-fields.

Similar insulin concentration enhancement behavior at different V_{pp} using FCS is shown in Figure 6, where AC-EO velocity increases with increasing AC-field strength. Insulin concentration increases more rapidly with increased V_{pp} as indicated by the steeper slope of time-dependent concentration profiles. As a result, the lag time decreases considerably from 2.5 h to 1.5 h to 1 h with increasing V_{pp} from 5 V to 10 V to 15 V, respectively. This is in spite of D remaining unchanged, confirming the monomer form of insulin without oligomerization prior to insulin aggregation.

The reduced lag time was also confirmed by CLSM measurements under the same experimental condition except for using 1% 5-CR6G labeled insulin in the buffer solution at 2.0 mg/ml total insulin concentration. Before the application of the AC-fields, the solution appeared homogeneous and featureless as shown in Figure 7(a). Using the same CLSM acquisition parameters such as optical pinhole size and detection gain, insulin aggregation under

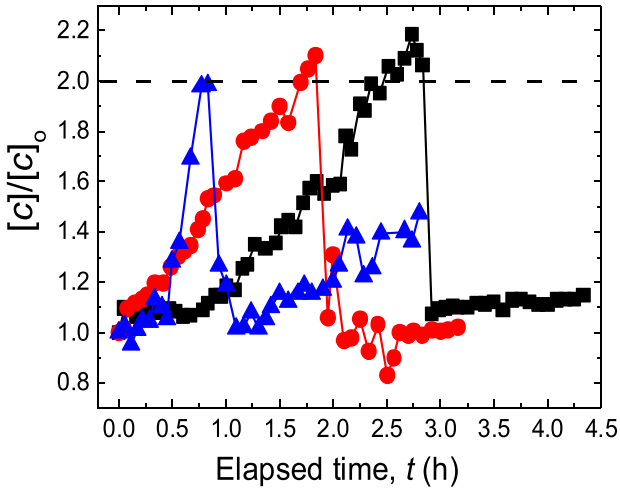

FIG. 6. Effect of applied voltage. $[c]/[c]_o$ as measured with FCS versus elapsed time under applied AC-fields of constant $\omega = 1$ kHz and $V_{pp} = 5$ V (black squares), 10 V (red circles), and 15 V (blue triangles).

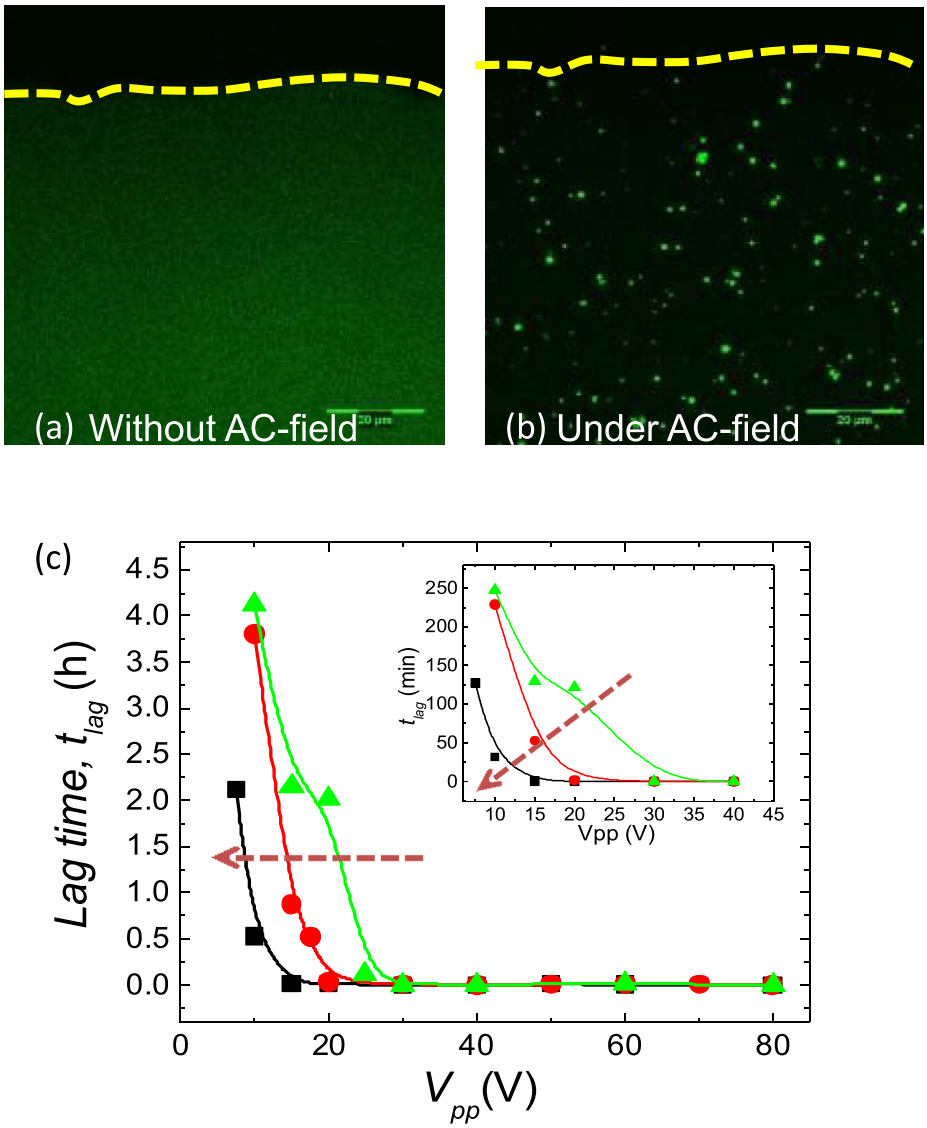

FIG. 7. Fluorescence micrographs of insulin aqueous solution near the edge of bottom electrode surface, depicted as a yellow dashed line (a) before and (b) after applied AC-field of $\omega = 2$ kHz and $V_{pp} = 20$ V. The detection gain set up for acquiring (b) is lower than that for (a) in order to improve the contrast. (c) Measured lag time for the onset insulin aggregation by CLSM versus V_{pp} at $\omega = 0.5$ kHz (black squares), 1 kHz (red circles), and 2 kHz (green triangles). Inset: the enlargement of the small V_{pp} range.

applied AC-fields with image acquisition at a time interval of 10 s over elapsed time was examined. As shown in Figure 7(b), fluorescent insulin aggregates after an elapsed time of about 2.5 h at $\omega = 2$ kHz and $V_{pp} = 20$ V appeared at the focal volume at the edge of the bottom electrode surface. The ω- and V_{pp}-dependent lag time determined by CLSM is summarized in Figure 7(c). Clearly, the measured lag time decreases rapidly from 2.5 h to <1 min as V_{pp} increased at three constant values of ω. It appears that at $V_{pp} > 30$ V, insulin aggregation occurs immediately upon the application of AC-fields, which is too fast to be detected by our CLSM, and thereby the lag time is noted approximately to be zero. The lag time determined from both CLSM and FCS measurements appears to show similar dependence on AC-electric field voltage and frequency. For both measurements, it appears that for the lower range of frequencies, $\omega = 0.5$–2 kHz, the lag time was shorter for the same applied V_{pp}, which overlaps with the $\omega_{AC\text{-}EO}$ for maximal AC-EO flow.

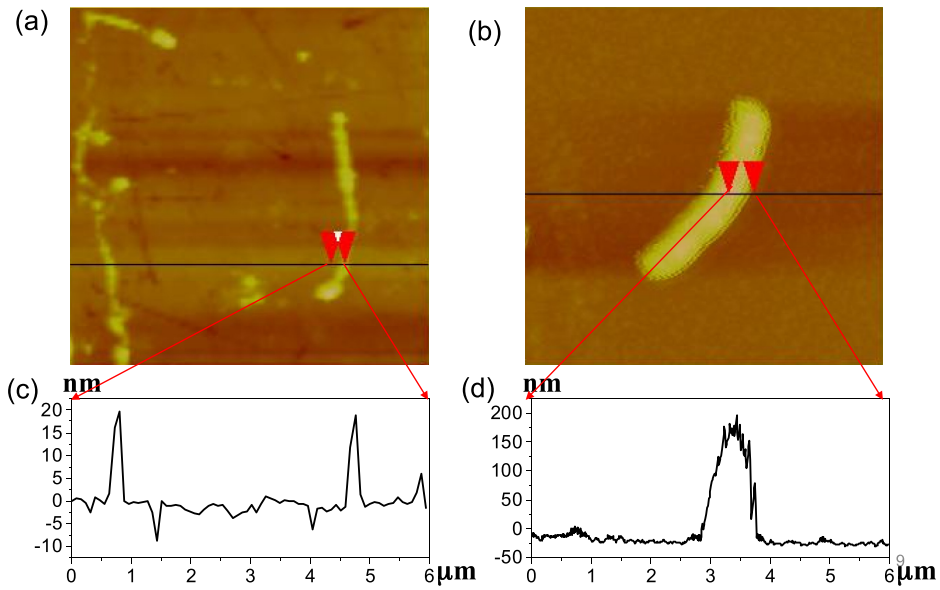

FIG. 8. AFM micrographs show fibril-like structure of insulin collected after 3 h exposure to applied AC-field of $\omega = 0.5$ kHz and V_{pp} = (a) 10 V and (b) 80 V over a scan area of $6 \times 6\ \mu m^2$. (c) and (d) are the section analysis of the line marked between two red arrows in (a) and (b), respectively.

We cautioned about the joule heating effect at high V_{pp} on insulin aggregation. The solution temperature at $V_{pp} < 60$ V remained constant at $T = 20 \pm 2\,^{\circ}C$; yet, the lag time under AC-fields is significantly reduced to <1 min in contrast to significantly longer lag time (>40 h[56]) without AC-fields at human body temperature $T = 37\,^{\circ}C$. Hence, we excluded the account of the joule heating for the significant acceleration of insulin aggregation under AC-fields. Furthermore, we observed no insulin accumulation on the bottom electrode surface. The resulting AC-field gradient across the large electrode gap spacing of 0.5 mm is sufficiently small and the size of insulin used in this work is about 1.2 nm in diameter, so AC-dielectrophoresis force imposed on insulin can be neglected.[53] Thus, it is confirmed that AC-EO flow can effectively mix and accumulate insulin in solution and consequently shorten the lag phase for accelerated insulin fibrillation, upon which no conversion from insulin monomer to oligomer is observed.

To obtain the structure of AC-field induced insulin aggregates, we used AFM to characterize the aggregates collected from the sample solution after being exposed to AC-fields over a time period longer than the lag time. As the AFM micrographs clearly show in Figure 8, insulin fibrils were detected from the samples collected after CLSM and FCS experiments. Insulin aggregation exposed to the AC-field of $\omega = 0.5$ kHz and $V_{pp} = 10$ V over 3 h clearly exhibits fibrillar nanostructure with an average length ~2–5 μm and ~20 nm in height (or diameter). For the same elapsed reaction time under an AC-field of $\omega = 0.5$ kHz, the fibrils were much thicker (~200 nm versus 20 nm) under $V_{pp} = 80$ V and 10 V, respectively, as evident from the AFM height profile.

CONCLUSIONS

The nucleation process of insulin fibrillation has been intensively studied by varying solution temperature,[1,52,56] pH,[25,52,57] and osmolytes.[9,58,59] In this work, we have taken a different approach by exploiting non-uniform AC-electric fields to control the nucleation kinetics of human insulin protein in aqueous buffer solution of constant pH = 2.74 and $T = 20\,^{\circ}C$. We have found that driven by AC-EO flow at the optimal frequency range of 0.5–2 kHz, insulin can be rapidly concentrated in a strong AC-field region near the electrode interface. Once the insulin concentration nearly doubled from its initial concentration, insulin aggregates were observed in the solution, leading to an abrupt reduction in the concentration of soluble insulin in aqueous

buffer solution. The measured lag time for the onset of insulin aggregation by both FCS and CLSM shows significant reduction from months in the absence of AC-fields to 0.5–3 h or even several minutes with increased AC-voltage at a frequency range of $\omega = 0.5$–$2\,\text{kHz}$ and at $T = 20\,^{\circ}\text{C}$.

The most surprising result from the AC-EO accelerated insulin fibrillation is the direct fibrillation from insulin monomers without the formation of oligomer precursors, which support the mechanism predicted by Ferrone.[14] The conversion from monomers to oligomer is a key step in several kinetic models of amyloid fibrillation.[51] The lack of oligomers with AC-field induced insulin aggregation appears to support that the fibrillation could simply involve the monomer re-conformation due to protein denaturation from a well-folded native conformation to β-sheet conformation. The action of AC-EO flow on rapidly concentrating insulin for accelerated nucleation process is equivalent to adding free insulin to growing fibrils. Due to the lack of an oligomeric precursor prior to insulin fibrillation, the application of non-uniform AC-fields could provide insight into biomedical engineering approaches to regulate the pathway and kinetics of amyloid fibrillation *in vitro*.

ACKNOWLEDGMENTS

We acknowledge the financial support from the National Science Foundation (NSF, CMMI-1129821 to Y.Z. and CTS-64-00610 to G.B.) for this work. We thank Dr. Arne Staby, Novo Nordisk A/S (Denmark), for supplying the human insulin.

[1]C. M. Dobson, Nature **426**(6968), 884–890 (2003).
[2]D. Eliezer, Science **336**(6079), 308–309 (2012).
[3]M. I. Ivanova, S. A. Sievers, M. R. Sawaya, J. S. Wall, and D. Eisenberg, Proc. Natl. Acad. Sci. U. S. A. **106**(45), 18990–18995 (2009).
[4]C. A. Ross and M. A. Poirier, Nat. Rev. Mol. Cell Biol. **6**(11), 891–898 (2005).
[5]M. Manno, E. F. Craparo, A. Podesta, D. Bulone, R. Carrotta, V. Martorana, G. Tiana, and P. L. San Biagio, J. Mol. Biol. **406**(2), 354–354 (2011).
[6]J. Adamcik and R. Mezzenga, Macromolecules **45**(3), 1137–1150 (2012).
[7]S. E. Hill, J. Robinson, G. Matthews, and M. Muschol, Biophys. J. **96**(9), 3781–3790 (2009).
[8]A. K. Buell, A. Dhulesia, M. F. Mossuto, N. Cremades, J. R. Kumita, M. Dumoulin, M. E. Welland, T. P. J. Knowles, X. Salvatella, and C. M. Dobson, J. Am. Chem. Soc. **133**(20), 7737–7743 (2011).
[9]D. A. White, A. K. Buell, T. P. J. Knowles, M. E. Welland, and C. M. Dobson, J. Am. Chem. Soc. **132**(14), 5170–5175 (2010).
[10]C. A. Ross and M. A. Poirier, Nat. Med. **10**(7), S10–S17 (2004).
[11]P. T. Lansbury and H. A. Lashuel, Nature **443**(7113), 774–779 (2006).
[12]L. N. Arnaudov and R. de Vries, Biophys. J. **88**(1), 515–526 (2005).
[13]T. P. J. Knowles, C. A. Waudby, G. L. Devlin, S. I. A. Cohen, A. Aguzzi, M. Vendruscolo, E. M. Terentjev, M. E. Welland, and C. M. Dobson, Science **326**(5959), 1533–1537 (2009).
[14]F. A. Ferrone, J. Mol. Biol. **427**(2), 287–290 (2015).
[15]M. Sunde and C. C. F. Blake, Q. Rev. Biophys. **31**(01), 1–39 (1998).
[16]J.–C. Rochet and P. T. Lansbury, Jr., Curr. Opin. Struct. Biol. **10**(1), 60–68 (2000).
[17]H. Levine, Protein Sci. **2**(3), 404–410 (1993).
[18]M. D. Kirkitadze, M. M. Condron, and D. B. Teplow, J. Mol. Biol. **312**(5), 1103–1119 (2001).
[19]J. C. Sacchettini and J. W. Kelly, Nat. Rev. Drug Discov. **1**(4), 267–275 (2002).
[20]A. M. Morris, M. A. Watzky, and R. G. Finke, BBA-Proteins Proteomics **1794**(3), 375–397 (2009).
[21]W.-F. Xue, S. W. Homans, and S. E. Radford, Proc. Natl. Acad. Sci. U. S. A. **105**(26), 8926–8931 (2008).
[22]M. Tanaka, S. R. Collins, B. H. Toyama, and J. S. Weissman, Nature **442**(7102), 585–589 (2006).
[23]A. M. Ruschak and A. D. Miranker, Proc. Natl. Acad. Sci. U. S. A. **104**(30), 12341–12346 (2007).
[24]F. Chiti and C. M. Dobson, Annu. Rev. Biochem. **75**, 333–366 (2006).
[25]D. M. Fowler, A. V. Koulov, W. E. Balch, and J. W. Kelly, Trends Biochem. Sci. **32**(5), 217–224 (2007).
[26]D. M. Fowler, A. V. Koulov, C. Alory-Jost, M. S. Marks, W. E. Balch, and J. W. Kelly, PLoS Biol. **4**(1), e6 (2006).
[27]A. Perálvarez-Marín, A. Barth, and A. Gräslund, J. Mol. Biol. **379**(3), 589–596 (2008).
[28]A. Nayak, C.-C. Lee, G. J. McRae, and G. Belfort, Biotechnol. Prog. **25**(5), 1508–1514 (2009).
[29]S. Wang, H.-C. Chang, and Y. Zhu, Macromolecules **43**(18), 7402–7405 (2010).
[30]D. Hou and H.-C. Chang, Appl. Phys. Lett. **92**(22), 223902 (2008).
[31]M. Dathe, K. Gast, D. Zirwer, and B. Mehlis, Diabetologia **30**(7), A511–A511 (1987).
[32]M. Dathe, K. Gast, D. Zirwer, H. Welfle, and B. Mehlis, Int. J. Pept. Protein Res. **36**(4), 344–349 (1990).
[33]M. Sorci, R. A. Grassucci, I. Hahn, J. Frank, and G. Belfort, Proteins **77**(1), 62–73 (2009).
[34]A. Nayak, M. Sorci, S. Krueger, and G. Belfort, Proteins **74**(3), 556–565 (2009).
[35]M. Muzaffar and A. Ahmad, PLoS One **6**(11), e27906 (2011).
[36]S. A. Kim, K. G. Heinze, and P. Schwille, Nat. Methods **4**(11), 963–973 (2007).
[37]C. L. Heldt, M. Sorci, D. Posada, A. Hirsa, and G. Belfort, Biotechnol. Bioeng. **108**(1), 237–241 (2011).
[38]N. G. Hentz, J. M. Richardson, J. R. Sportsman, J. Daijo, and G. S. Sittampalam, Anal. Chem. **69**(24), 4994–5000 (1997).

[39]M. Kinjo and R. Rigler, Nucl. Acids Res. **23**(10), 1795–1799 (1995).
[40]M. Pitschke, R. Prior, M. Haupt, and D. Riesner, Nat. Med. **4**(7), 832–834 (1998).
[41]E. L. Elson and D. Magde, Biopolymers **13**(1), 1–27 (1974).
[42]V. E. Goodrich, E. Connor, S. Wang, J. Yang, J. Zhao, and Y. Zhu, Soft Matter **9**(20), 5052–5060 (2013).
[43]R. Rigler, S. Wennmalm, and L. Edman, *Fluorescence Correlation Spectroscopy* (Springer, Berlin, 2001), Vol. 65, pp. 459–476.
[44]R. H. Kohler, P. Schwille, W. W. Webb, and M. R. Hanson, J. Cell Sci. **113**(22), 3921–3930 (2000), http://jcs.biologists.org/content/113/22/3921.abstract.
[45]C. B. Müller, A. Loman, V. Pacheco, F. Koberling, D. Willbold, W. Richtering, and J. Enderlein, Europhys. Lett. **83**(4), 46001 (2008).
[46]L. F. Pease Iii, M. Sorci, S. Guha, D.-H. Tsai, M. R. Zachariah, M. J. Tarlov, and G. Belfort, Biophys. J. **99**(12), 3979–3985 (2010).
[47]S. Hvidt, Biophys. Chem. **39**(2), 205–213 (1991).
[48]V. Banerjee and K. P. Das, Colloids Surf., B **92**(0), 142–150 (2012).
[49]E. Helmerhorst and G. B. Stokes, Diabetes **36**(3), 261–264 (1987).
[50]F. Librizzi and C. Rischel, Protein Sci. **14**(12), 3129–3134 (2005).
[51]C.-C. Lee, A. Nayak, A. Sethuraman, G. Belfort, and G. J. McRae, Biophys. J. **92**(10), 3448–3458 (2007).
[52]L. Nielsen, R. Khurana, A. Coats, S. Frokjaer, J. Brange, S. Vyas, V. N. Uversky, and A. L. Fink, Biochemistry **40**(20), 6036–6046 (2001).
[53]T. B. Jones, *Electromechanics of Particles* (Cambridge University Press, 1995).
[54]S. Wang and Y. Zhu, Biomicrofluidics **6**(2), 024116 (2012).
[55]N. G. Green, A. Ramos, A. González, H. Morgan, and A. Castellanos, Phys. Rev. E **61**(4), 4011–4018 (2000).
[56]A. Arora, C. Ha, and C. B. Park, Protein Sci. **13**(9), 2429–2436 (2004).
[57]W. Kadima, L. Ogendal, R. Bauer, N. Kaarsholm, K. Brodersen, J. F. Hansen, and P. Porting, Biopolymers **33**(11), 1643–1657 (1993).
[58]T. P. J. Knowles, W. Shu, G. L. Devlin, S. Meehan, S. Auer, C. M. Dobson, and M. E. Welland, Proc. Natl. Acad. Sci. U. S. A. **104**(24), 10016–10021 (2007).
[59]B. Murray, J. Rosenthal, Z. Zheng, D. Isaacson, Y. Zhu, and G. Belfort, Langmuir **31**(14), 4246–4254 (2015).